Adsorption (2022) 28:219–230
https://doi.org/10.1007/s10450-022-00364-w

Comment on the applicability of the Gurvich rule for estimation of pore volume in microporous zeolites

Amir H. Farmahini[1] · Khalid Limbada[1] · Lev Sarkisov[1]

Received: 8 April 2022 / Revised: 25 July 2022 / Accepted: 26 July 2022 / Published online: 25 August 2022

Abstract
This comment seeks to establish a relation between two definitions of the pore volume of a microporous crystalline material. According to the first definition based on the Gurvich rule, the volume of the pores can be estimated from the saturated amount of vapour adsorbed, using the bulk liquid density of adsorbate as the conversion factor. The second definition is based on a purely geometric consideration of the porous space. With argon as the adsorbate and all-silica zeolite structures from the International Zeolite Association (IZA) database as the model adsorbents, we generate adsorption data using Grand Canonical Monte Carlo simulations and structural characteristics of the materials from the Poreblazer PB4.0 software. Under confinement in zeolitic pores, adsorbed argon forms structures very different from the liquid-like configurations. However, the pore volumes of these materials obtained from the Gurvich may deviate positively or negatively from the reference geometric value. Considering simply the geometric features of the materials, such as the pore volume itself or the pore size distribution, it proved to be difficult to anticipate how the volume from the Gurvich rule would deviate from the geometric volume for a particular structure. Overall, volume from the Gurvich rule agrees with the geometric volume within 25% error for 82% of the structures from the IZA database. As an additional outcome of this study, we provide a comprehensive database of textural characteristics and simulated argon adsorption data for all-silica zeolites, which can be used as reference values for the assessment of the quality of the microporous samples of all-silica zeolites in future experimental studies.

Keywords Pore characterization · Adsorption · Molecular simulation

1 Introduction

The specific volume of pores is one of the key properties of an adsorbent material. It defines its adsorption behaviour and functionality in applications such as gas storage, separations and drug release. Hence, accurate and consistent estimation of the pore volume of real and hypothetical materials is vital for their systematic screening for a specific adsorption application.

In experiments, the pore volume of an adsorbent is typically obtained using physical adsorption characterization techniques, such as adsorption of nitrogen at 77 K or argon at 87 K. From these measurements, pore volume is estimated according to the Gurvich rule [1]:

$$V_{p,G} = \frac{m_{ads.}^{Sat.}}{\rho^{liq.}} \tag{1}$$

Here, V_p, $m_{ads.}^{Sat.}$ and $\rho^{liq.}$ are the total pore volume, adsorption uptake at saturation, and density of liquid fluid, respectively. The key assumption of the Gurvich is that fluid adsorbed in the pores has the same density as the bulk liquid at the same temperature and pressure. In practice, it is often challenging to identify the plateau of the adsorption isotherm where the Eq. (1) can be applied, because of the presence of the mesopores in the actual sample of the material and also because of the adsorption on the external surface. In this case, application of α_s-plot method is recommended [2]. Using experimental data, it is also possible to estimate pore volume by integrating over the pore size distribution, which in turn is obtained by from the Non-Local Density Functional Theory (NLDFT). However, the Gurvich rule approach still represents common and recent practice [3]. We therefore, for now, leave the NLDFT approach and other

✉ Lev Sarkisov
Lev.Sarkisov@manchester.ac.uk

[1] Department of Chemical Engineering, School of Engineering, The University of Manchester, Manchester M13 9PL, UK

methods, their applicability and pitfalls outside of the scope of this article.

Alternatively, as has been recently discussed by Ongari et al. [4], one can introduce a purely mathematical definition of the volume of the pores inside a given crystal structure. Depending on the definition, various computational techniques can be employed to obtain the value of this property. Indeed, computational structure characterization methods for textural properties of porous materials, such as pore volume and surface area, have gained much attention in recent years as a way to compare and classify porous structures [5–10]. These computational approaches became particularly important for the families of porous materials such as zeolites and Metal–Organic Frameworks (MOFs), where not only a large number of them have been already discovered in the experiments, but many more materials have been hypothesized to exist using computational methods [10–13].

Hence, we have two alternative ways to define the pore volume: one based on the experimental technique and physical phenomena in a real sample, and the other based on the mathematical concepts of the volume confined inside some geometrical structures. The question we are posing here is: what is the relation between the pore volume obtained using the Gurvich rule and the mathematical definition of this property? To understand the importance of this question, let us for a moment assume that the two properties have exactly the same meaning and give exactly the same value for the pore volume for a perfect crystal of a particular material. This equivalency would provide a powerful tool for the assessment of the quality of the real, experimental sample of this material: any deviation from the reference value obtained for the perfect crystal structure would point to the presence of defects and impurities. Interestingly, recently values of the pore volume have been used to provide a more accurate way to confirm identity of MOFs across different databases [14].

Despite several key contributions to the topic [3, 14], we believe this link is not yet fully established. To understand the current progress and developments, it is useful to briefly mention different mathematical concepts of the pore volume as depicted in Fig. 1, which have been also discussed by Ongari et al. [4].

Depending on the molecular probe, we can distinguish the geometrical volume, defined as the volume accessible to

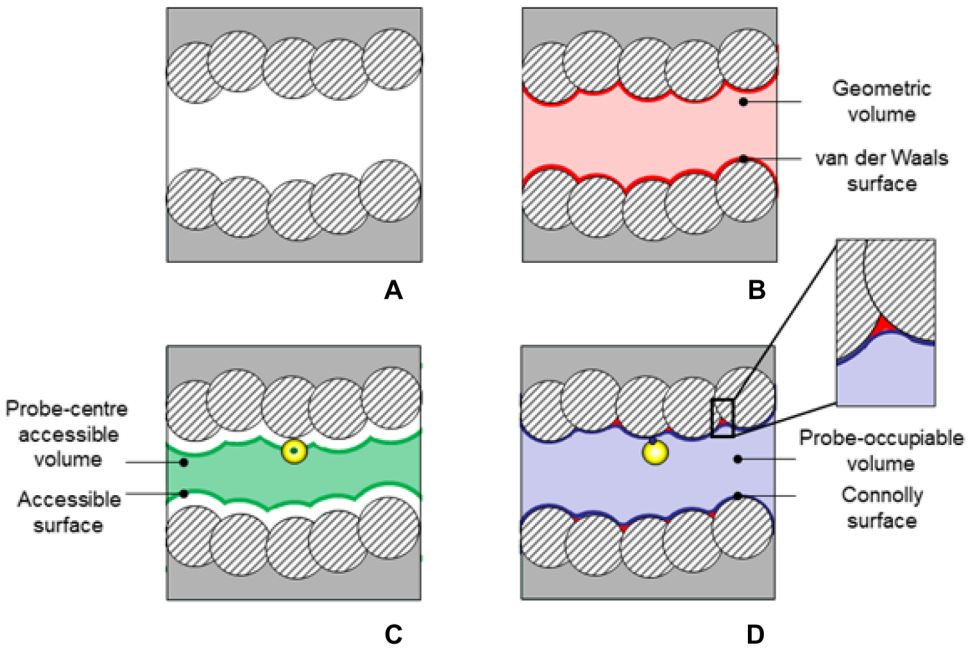

Fig. 1 Schematic depiction of different definitions of pore volume: **A** A model system consisting of a material, shown as the area shaded in grey, and a pore spanning the system in the horizontal direction. Atoms of the material at the boundary between the shaded area and the pore are shown as striped circles. **B** The geometric pore volume is defined as the region of the system not occupied by atoms (shown in light red). The boundary between the occupied and empty space is the van der Waals surface, shown in **B** as the red line. **C** Schematic depiction of the accessible surface: it is the surface formed by the centre of the probe particle rolling over the surface of the atoms of the structure, shown as the green line. A region of space enclosed by the accessible surface corresponds to the probe-centre accessible probe volume, shown as the green shaded area. **D** Schematic depiction of the Connolly surface: it is the surface formed by the tip of the probe particle rolling over atoms of the structure, shown as the dark blue line. A region of space enclosed by the Connolly surface corresponds to the probe-occupiable volume shown as the blue shaded area. The difference between the geometric volume and the probe-occupiable volume is shown as residual red-shaded areas in panel D (see the inset for more details). (Reprinted with permission from Sarkisov et al., Chem. Mater. 2020, 32, 9849–9867. Copyright 2020 American Chemical Society) (Color figure online)

a point (zero-size probe); probe-centre accessible volume, defined as the volume enclosed by the accessible surface, which can be seen as the surface formed by tracing the centre of the probe particle rolled on the surface of the atoms of the structure; and probe-occupiable volume, defined as the volume enclosed by the Connolly surface, which is formed by the outer edge of the probe particle rolling over the atoms of the structure.

By looking at the definitions of these geometric properties, one can immediately identify several inconsistencies with what is measured experimentally, even on the ideal crystal. Firstly, physical adsorption characterization methods commonly use non-spherical probes, such as nitrogen and carbon dioxide. These molecules, upon adsorption, may form packings or prefer particular orientations, leading to the different volume of the pore space, as "observed" by a particular probe. Secondly, these definitions assume that the atoms of the structure can be approximated as spheres. A more accurate representation of the walls of the structure would involve calculating the electron density using, for example, quantum–mechanical DFT methods, and treating the walls as electron density isosurface.

In an alternative computational approach to obtain the pore volume we can imitate the experimental helium porosimetry procedure, where the volume of the pores is measured by the amount of helium present in the pores at room temperature and assuming that helium is not adsorbing, in other words, its density remains uniform ideal gas-like density throughout the volume of the pores. Previously, it has been shown that this is not the case, and helium does adsorb to some extent. In the computational procedure, the volume of the pores is estimated by calculating the second virial coefficient of helium at room temperature using, for example, the Widom insertion method. In reality helium does interact with the walls, and does adsorb to some extent as has been discussed previously by Brandani et al. [15]. In result, the volume obtained in this fashion can be very different from the geometric volume or volume obtained from argon or nitrogen sorption at the cryogenic temperatures. In fact, this helium volume can deviate both positively and negatively from the reference geometric volume as has been demonstrated by Ongari et al. [4]. For these reasons, we leave this property outside of further discussion in this article, although it is reported in the Table S1 of the Supporting Information.

Finally, we should also distinguish network-accessible properties vs total properties. Depending on the size of the probe molecule with which a particular property is obtain, presence of the narrow windows in the structure with the diameter smaller than the size of the probe can make some of the regions of the porous space inaccessible to the probe. This is illustrated in Fig. 2. In experiments, the isolated, closed pores would not be accessed by the adsorbate molecules, and to make comparison of the geometric properties and experimental results consistent, we should consider network-accessible geometric properties (e.g. network-accessible probe-occupiable volume, etc.). If the network effects are not taken into account or do not play a role, then the properties obtained for all the porosity available are called the total properties (e.g. total probe-occupiable volume, etc.).

We refer the reader to the recent article by Sarkisov et al. for a more comprehensive discussion of these properties and the algorithms associated with their calculation [7].

In a recent article published by [4], it was demonstrated that it is the probe-occupiable volume that is the most relevant property in application to the adsorption problems. More recently, the authors also compared experimentally measured values of the pore volume against calculated values of this property based on the perfect crystal structure of 291 MOFs [14]. In their new study, they showed that the measured and computed values of pore volume agree only in 35% of the cases (within 10–25% error). Recently, Islamoglu

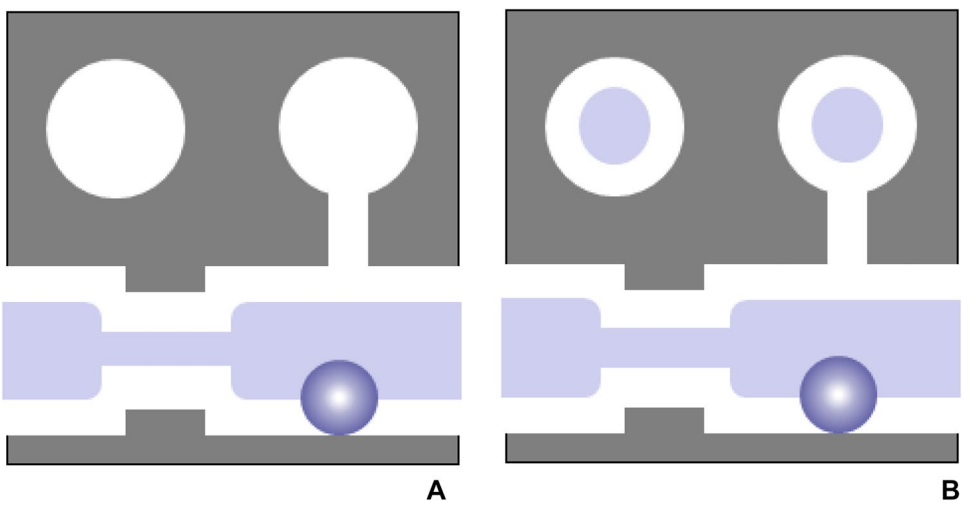

Fig. 2 Schematic illustration of the network-accessible (**A**) and total (**B**) probe-centre accessible volumes, shown as areas shaded in light blue. In panel **A**, the cavities are accessible to the probe particle shown in blue. In panel **B** the same property is calculated for all pores in the system, regardless of their physical accessibility to the probe. (Adapted from Sarkisov et al., Chem. Mater. 2020, 32, 9849–9867. Copyright 2020 American Chemical Society) (Color figure online)

et al. measured pore volume of 9 MOFs using adsorption of 5 different probe molecules namely nitrogen, argon, krypton, oxygen, and carbon dioxide using the Gurvich rule and compared the results from the computational methods, using the probe-occupiable definition of the pore volume [3]. According to their results, despite a reasonable average error of 16.65%, individual errors for different materials vary from 0.58 to 55.71%.

We can identify the following reasons for the disagreement between the experimentally measured values of pore volume and their computational counterparts, observed in the reviewed studies. Firstly, the Gurvich method assumes that fluid under confinement has the same density as the bulk liquid under the same temperature and pressure. Intuitively, we anticipate that this assumption must break down for the very small pores (in the microporous regime), as the very structure of the pores may impose the packing order on the confined molecules that is very different from their arrangement in the liquid state. This should result in the departure of the values of the pore volume obtained from the Gurvich rule from the geometric definition of the pore space, which is agnostic about the molecular packing scenarios. Secondly, in the computational structure characterization tools a model of the probe molecule is used which only approximates physical properties of the corresponding actual probe species (e.g. argon or nitrogen). Finally, and most importantly, the experimental measurements are carried out on real samples of materials, featuring various defects, while computational studies are performed using the ideal crystal structure. Hence, the experimental and computational approaches are not consistent with each other as they calculate the required property for, effectively, two different structures. Aside from fundamental differences in the methodology and the underlying assumptions of the experimental and computational methods, conflating experimental and simulation data prevents us from isolating the specific differences between the predictions of the Gurvuch rule and the geometrical volume.

In fact, the above problem defines the remit of the current article. To circumvent the issue of the consistency between the two aforementioned approaches, here we replace the experimental studies on the real samples with molecular simulations of adsorption on ideal crystal structures. We focus specifically on argon at 87 K, as this is a spherical probe consistent with the geometric methods. More complex effects associated with packing and orientation of non-spherical probes, such as nitrogen, are left outside of the scope of this study. The Gurvich rule is then applied to extract the corresponding pore volume from the simulated isotherm. In the current study, we focus on zeolite topologies that have been realized experimentally and approved by the Structure Commission of the International Zeolite Association (IZA-SC). Our selection of the database of materials (zeolites as opposed to, for example, MOFs) is justified on the following grounds: Compared to MOFs, zeolites tend to be more microporous (the average pore size is shifted to lower values) and this is the regime that is likely to pose a significant challenge for the Gurvich rule. Moreover, we only focus on all-silica structures of the IZA database. This creates less of a chemical heterogeneity in the structures under consideration, which in turn allows the use of simpler molecular forcefields with fewer interaction parameters in molecular simulation, compared to more chemically heterogeneous MOFs. Finally, zeolites are already extensively used in various applications on industrial scale and accurate estimation of their reference pore volumes is of a direct, practical importance [16–18].

The database of Zeolite Structures was originally designed and implemented by Baerlocher and McCusker in 1996 on behalf of IZA-SC. The number of topologies collected in the database has increased from 98 in 1996 to 255 in 2021 which now includes 244 fully ordered and 11 partially disordered framework types [19]. The zeolites collected in IZA-DZS were previously characterized by Floudas et al. in 2011 to provide insights about selectivity of various zeolite frameworks [5]. The results were made available online as part of the freely available ZEOMICS web tool. ZEOMICS reported on textural properties of 194 zeolite topologies that were available at the time of its publication. It also contained information regarding pore occupancy of zeolites as a function of molecular size of the adsorbing molecules.

While focusing on the applicability of the Gurvich rule as the main scientific topic of the article, we use this opportunity to revisit the updated Database of Zeolite Structures to calculate the full spectrum of properties available within the PoreBlazer tool [8]. We make these properties along with the required simulation details available to the public through our group GitHub depository.

2 Computational details

All zeolite frameworks published by the International Zeolite Association until December 2021 are collected from the IZA database, which include 244 fully ordered and 11 partially disordered framework types [19]. Pore structure characterization has been performed for fully silica version of all zeolite topologies using PoreBlazer v4.0 [7]. The results include theoretical values of total and accessible pore volumes and surface areas (using argon probe), largest cavity diameter, pore limiting diameter, porosity, and network percolation. In the context of this study, we are particularly interested in the probe-occupiable pore volume. Table S1 of the Supporting Information provides the entire body of data obtained from our characterization study of the IZA-DZS database.

We employ grand canonical Monte Carlo (GCMC) simulation technique to calculate saturation capacity of each zeolite for argon at 87 K. The modified Lennard–Jones equation of state [20] was used to obtain the saturation pressure of the argon model at this temperature (83 kPa), with GCMC simulations performed somewhat above the saturation pressure (101 kPa) to ensure adsorption saturation is fully achieved. As a reference, we performed an NPT simulation of the bulk phase of the employed model of argon at 87 K and 101 kPa and the obtained density of 1.4 g/cc is in excellent agreement with the prediction from the revised Lennard–Jones equation of state. GCMC simulations are performed using RASPA v.2.0.37 [21]. Each simulation is performed for 2×10^5 MC cycles, and the number of cycles for both equilibration and production stages of the simulations are equal. In these simulations each cycle consists of N Monte Carlo trial moves where N is equal to the average number of argon molecules in the framework. 12–6 Lennard–Jones potential is used to model intermolecular interactions in both RASPA and PoreBlazer. Details of force field and other simulation parameters used in the simulations are provided in Table 1. We note here that while other choices of the force fields parameters are possible (e.g. by Talu and Myers [22]), the experimental studies for argon adsorption in pure silica zeolites at 87 K are still scarce to validate them. Here, the main emphasis is on the consistency of the parameters used for the geometric probe in PoreBlazer and for adsorbate in GCMC simulations.

3 Results and discussion

The main objective of this study is to probe the applicability and accuracy of the Gurvich rule for estimation of the total pore volume in microporous zeolites by comparing this property to the probe-occupiable volume ($V_{p,PO}$), defined in Fig. 1. Before we consider the actual results obtained for the zeolite frameworks from the IZA-DZS database, it is instructive to explore how and why the volume observed from the Gurvich rule ($V_{p,G}$) would deviate from $V_{p,PO}$. Indeed, in Fig. 3 we schematically depict possible scenarios in pores of simple geometry, with the red line indicating the boundaries of the probe-occupiable volume. Let us start with panel *A* of this figure, which shows a cross-section of a cylindrical pore with a fairly large diameter. Here, the fluid particles pack in an arrangement resembling the liquid structure. A valuable characteristic of this packing is its volume fraction. As has been recently proved analytically by Zaccone, random close packing of equal hard spheres has volume fraction of $\phi_{RCP} = 0.65896$ [23]. This can be contrasted with the highest theoretical packing of equal hard spheres, such as the FCC packing

Table 1 Force field and other simulation parameters used for structural characterization and GCMC simulation

Atom	σ (Å)	ε (K)	Cut-off distance (Å)	Temperature (K)	Pressure (atm)	References
He	2.580	10.22	12.8	298	–	Hirschfelder et al. [32]
Ar	3.400	119.80	12.8	87	1	Hirschfelder et al. [32]
Si	3.826	202.15	12.8	–	–	Rappe et al. [33]
O	3.118	30.20	12.8	–	–	Rappe et al. [33]

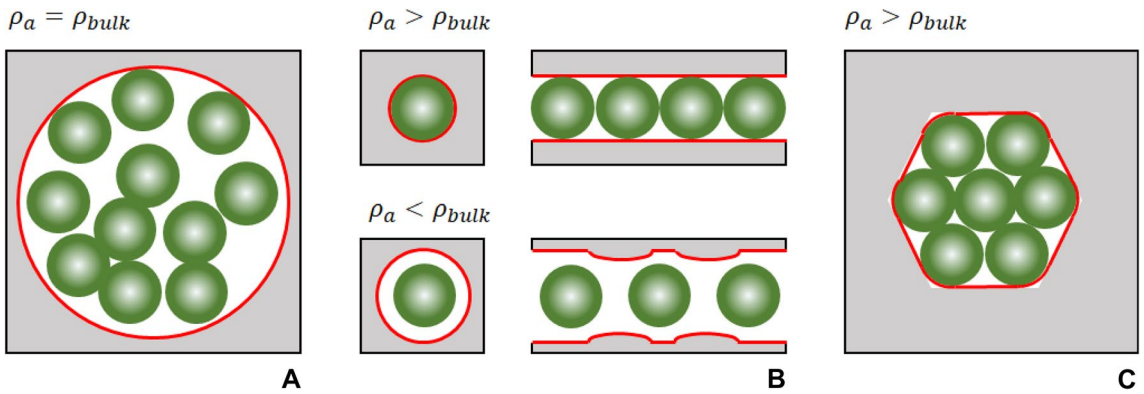

Fig. 3 Schematic depiction of the fluid particle packing scenarios in one-dimensional channels. **A** liquid-like packing in a large diameter channel with adsorbed density ρ_a equal to the bulk density ρ_{bulk}; **B** string-like packings in a narrow pore. Here, depending on the diameter of the pore and the molecular packing, adsorbed density can be lower $\rho_a < \rho_{bulk}$ or higher $\rho_a > \rho_{bulk}$ compared to the bulk density; **C** commensurate FCC/HCP packing in a hexagonal channel, $\rho_a > \rho_{bulk}$

with $\phi_{FCC} = 0.74048$. In case of panel *A*, the density of the fluid is expected to be equal or close to the liquid density and the volume obtained from the Gurvich rule ($V_{p,G}$) should be equal to the probe-occupiable volume ($V_{p,PO}$). Several alternative scenarios are depicted in panel *B*. Let us first consider close packing of particles in a cylinder of the same diameter as the particles (top schematics in panel *B* of Fig. 3). In this case, $\phi_{cyl} = \frac{2}{3}$, or 0.66667. This is slightly higher than the value for the random close packing in three dimensions. The density of the fluid adsorbed in a channel like this one should also be higher than the density of the bulk liquid. At the bottom of panel *B*, we show a situation where the diameter of the channel is slightly larger than the diameter of the fluid particle. The adsorbed fluid particles form a chain and cannot arrange themselves in a way that they can occupy the whole volume available. This chain may also feature gaps between the adsorbed particles, as shown in the schematic. In this case, $V_{p,PO}$ is larger than $V_{p,G}$ and the density of fluid particles in the pore is lower than the density of the corresponding liquid. As has been systematically shown by Schmidt and Lowen [24] and by Oğuz et al. [25] in channels of simple geometry, packings of hard spheres have lower density and phase volume fraction than ordered close packing. Finally, in panel *C* we show a channel with hexagonal cross-section. The dimensions of these channel are commensurate with the FCC or HCP packing of fluid particles, as shown in the schematics. The FCC packing has higher density than the liquid and hence in this case the volume obtained from the Gurvich rule would exceed the actual $V_{p,PO}$, enclosed by the red line. Of course, in real materials we can also imagine a combination of these scenarios. For example, ordered FCC clusters connected by chains of particles or regions of low density may result in the average density being close to the liquid density of the same fluid.

We now turn our attention to the parity plot shown in Fig. 4, which compares theoretical probe-occupiable pore volume ($V_{p,PO}$) of zeolites from IZA-DZS database with the values of total pore volume estimated using Gurvich rule ($V_{p,G}$) based on simulated adsorption of argon at 87 K. We note that for the estimation of $V_{p,G}$ from Eq. (1), we use the liquid density of argon model that is employed in our GCMC simulation. This is equal to 1.4 cc/g which is the same as the density of liquid argon from experiment (1.397 g/cc) [26].

As shown here, no obvious correlation can be observed between the accuracy of the Gurvich rule and the magnitude of pore volume reported. In fact, good agreement is observed for both classes of materials with small and large pore volumes. The deviations between the reported values of $V_{p,G}$ and $V_{p,PO}$ can be further quantified by the statistical measures such as the relative error $\left(\frac{|V_{p,G}-V_{p,PO}|}{V_{p,PO}} \times 100\%\right)$, reported in Table S1 of the SI, Root Mean Squared

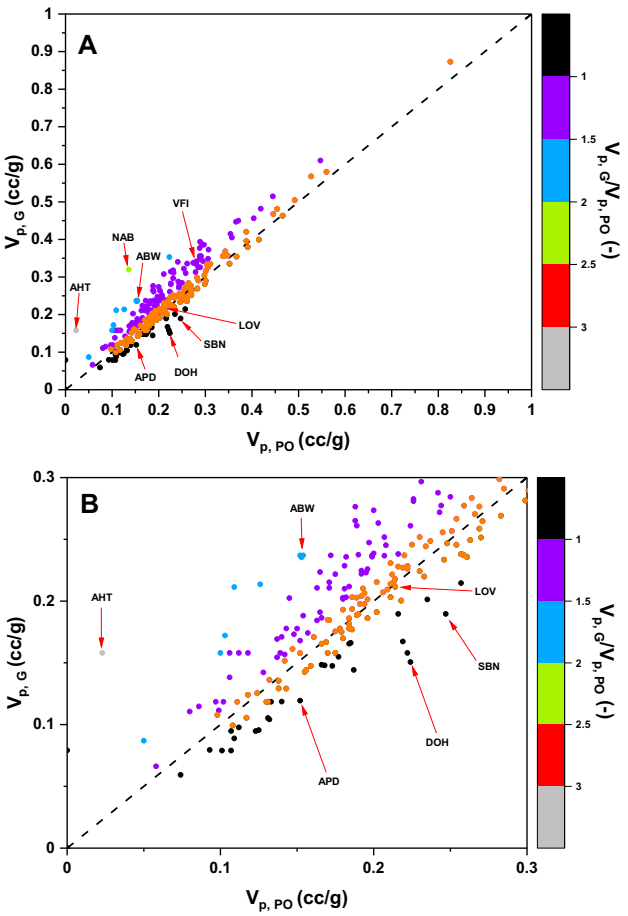

Fig. 4 Comparison of probe-occupiable pore volume ($V_{p,PO}$) and the pore volume estimated using the Gurvich rule ($V_{p,G}$) for all zeolites (**a**), and for zeolites with $V_{p,G}$ and $V_{p,PO} < 0.3 cc/g$ (**b**). Data points are colour-coded based on the ratio of $\frac{V_{p,G}}{V_{p,PO}}$. Orange colour (superimposed on the original data) indicates zeolites in which $\frac{V_{p,G}}{V_{p,PO}} \approx 1$ (within 10% of the relative error, defined in the text)

Deviation (RMSD), defined as $RMSD = \sqrt{\frac{\sum_{i=1}^{N}(\{V_{p,G}\}_i - \{V_{p,PO}\}_i)^2}{N}}$ and Mean Signed Deviation (MSD), defined as $MSD = \frac{\sum_{i=1}^{N}\{V_{p,G}\}_i - \{V_{p,PO}\}_i}{N}$. Here, N is the number of materials under consideration and i corresponds to the properties of the individual material. The obtained values of RMSD and MSD are 0.042 and 0.021, respectively. Consistent with what is shown in Fig. 4, a positive value of MSD shows that the Gurvich rule overall overestimates the pore volume calculated by the geometric approach.

Intuitively, one would expect to see better agreement between $V_{p,PO}$ and $V_{p,G}$ for materials with larger pore volumes, considering materials with larger pore volumes are more likely to contain larger pores, although this is not always guaranteed. In fact, it is striking to see that there

are many examples of good agreement between $V_{p,PO}$ and $V_{p,G}$ for materials with very small pore volumes as shown in Fig. 4b. To take a closer look into the information provided in Fig. 4, we have also calculated relative frequency of the ratios between $V_{p,PO}$ and $V_{p,G}$ for the materials studied here. The results are plotted in Fig. 5.

As shown in Fig. 5a, $\frac{V_{p,G}}{V_{p,PO}}$ between 0.75 and 1.25 constitute more than 80% of the frequency spectrum, an indication of good accuracy of Gurvich rule for estimation of total pore volume. However, considering most of the materials in IZA-DZS database have pore volumes smaller than 0.3 cc/g, we see little difference when comparing this picture with that shown in Fig. 5b where only zeolites with small pore volumes ($V_p < 0.3cc/g$) are considered. It would be therefore, interesting to find out why the Gurvich rule is able to provide an accurate estimation of pore volume for a wide range of materials with both small and larger pore volumes.

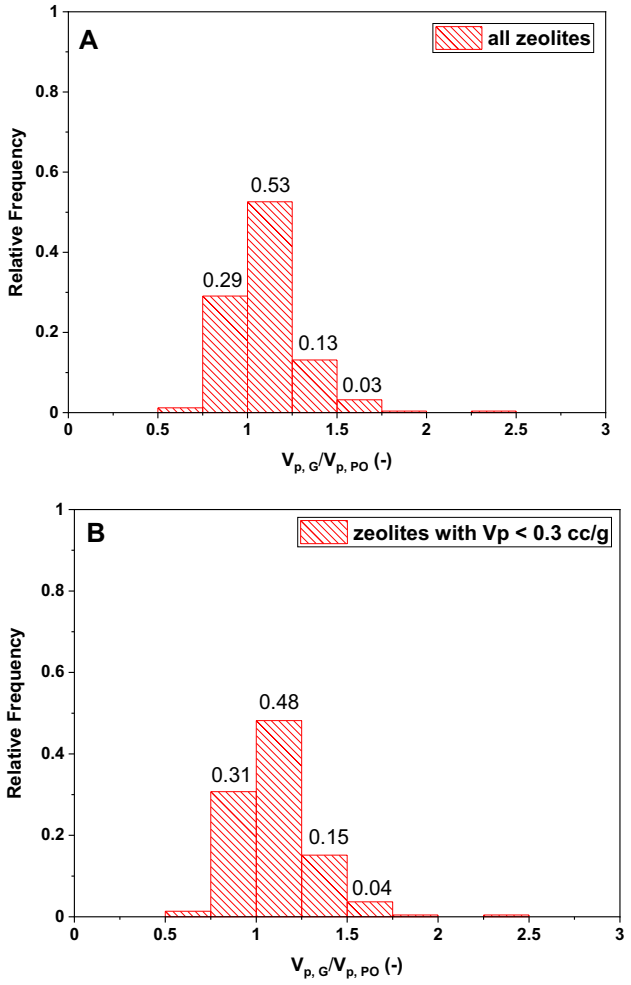

Fig. 5 Distribution of $\frac{V_{p,G}}{V_{p,PO}}$ for all IZA zeolites (except AHT) (**a**), and for zeolites with $V_p < 0.3cc/g$ (**b**). The numbers on the top of the bars indicate their actual values

To answer this question, let us initially explore in more detail the materials with the most significant differences between the Gurvich rule predictions ($V_{p,G}$) and the probe-occupiable volume ($V_{p,PO}$). In Table 2, these materials are classified in two distinct groups. The first 10 materials from the top exhibit the highest negative deviation ($V_{p,G} < V_{p,PO}$) which means the Gurvich rule underestimates $V_{p,PO}$. The bottom 10 materials correspond to the highest positive deviations observed in the IZA-DZS database ($V_{p,G} > V_{p,PO}$), where the Gurvich rule predicts higher pore volume compared to $V_{p,PO}$. In the table, we show only a selection of properties, whereas the complete set of properties is reported in Table S1 of the SI.

Analysis of the properties and computer visualizations of the materials in Table 2 reveals several interesting trends. For the materials with negative deviations most of the materials (APD, ATV, AWO, CAS, SBN, UOZ) feature rather narrow channels (< 5 Å), as seen from their pore size distributions shown for several selected materials in Fig. 6a.

Within these channels, adsorbed argon molecules form loose strings. An example of these materials is shown in Fig. 7a for APD zeolite, while molecular visualizations of argon packing in all other zeolites from this group are provided in Fig. S2 of the SI. These materials seem to clearly follow scenario in the lower schematics of the panel *B* in Fig. 3. Other materials (DOH, SOD, MTN) feature larger LCD cages (> 5 Å) and argon is observed as small clusters of two or more atoms, and in some cases additional atoms in between the cages (e.g. materials MEP, MTN, SOD, and DOH). In the SBN material, separate argon atoms are located in individual cages connected by some passages.

In the case of materials with positive deviations ($V_{p,G} > V_{p,PO}$) in Table 2, they all feature very narrow pores with LCD not exceeding 4.5 Å as illustrated in Figs. 6b and S2(b) of the SI. Interestingly, many materials in this group also feature one dimensional channels and strings of adsorbed argon atoms, including ABW, CHI, GOO, NSI. Adsorption in some other structures from this group can also be considered as string-like, however with strings much more twisted to follow the tortuous nature of the channels. As an example of a string-like packing with a strong positive deviation, we visualize ABW in Fig. 7. More examples of materials from this group are illustrated in Fig. S3 of the SI.

By comparing APD and ABW topologies in Fig. 7, it seems the crucial difference between the two structures, one with a strong negative deviation and another one with a strong positive deviation, is associated with molecular packing of argon atoms inside the channels, and this in turn depends on the structural characteristics of the channel.

We have compared PSDs of these two topologies in Fig. 8. From the pure LCD, PLD and PSD analysis, it is not

Table 2 Zeolites with largest deviation between $V_{p,PO}$ and $V_{p,G}$

Zeolite	PLD (Å)	LCD (Å)	$V_{p,PO}$ (cc/g)	Argon uptake (g/g)	$V_{p,G}$ (cc/g)	Relative error (%)	$\frac{V_{p,G}}{V_{p,PO}}$
DOH	2.240	7.310	0.224	0.211	0.151	32.746	0.673
SOD	2.050	5.790	0.222	0.222	0.158	28.833	0.712
CAS	2.540	4.550	0.107	0.111	0.079	26.172	0.738
MTN	2.070	6.770	0.219	0.235	0.167	23.614	0.764
AWO	3.260	4.610	0.125	0.134	0.096	23.573	0.764
SBN	3.230	4.570	0.247	0.266	0.190	23.243	0.768
UOZ	0.860	4.860	0.123	0.133	0.095	22.931	0.771
MEP	1.490	4.870	0.187	0.202	0.144	22.859	0.771
ATV	3.070	4.220	0.101	0.111	0.079	21.786	0.782
APD	3.120	4.420	0.152	0.167	0.119	21.482	0.785
AHT	2.290	3.470	0.023	0.222	0.158	586.920	6.869
NAB	3.020	3.820	0.136	0.449	0.320	135.245	2.352
VNI	2.280	4.290	0.109	0.297	0.211	93.935	1.939
CHI	2.960	3.420	0.050	0.122	0.087	73.945	1.739
YUG	2.650	4.010	0.126	0.300	0.214	69.493	1.695
GOO	2.650	4.010	0.103	0.241	0.172	67.131	1.671
ACO	3.040	4.050	0.223	0.495	0.353	58.221	1.582
NSI	2.570	3.630	0.100	0.222	0.158	57.992	1.580
MON	2.970	3.760	0.152	0.332	0.237	55.913	1.559
ABW	3.090	3.730	0.154	0.332	0.237	53.888	1.539

The first 10 materials exhibit the highest negative deviation, and the bottom 10 materials correspond to the highest positive deviations

evident why the structures would behave so differently. However, one conjecture that is possible to construct is that we should then see string-like structures among zeolite topologies in which adsorbed phase happens to have density very close to that of the liquid argon. Indeed, we can identify structures such as LOV, which also feature one dimensional (although tortuous) channels with PLD = 3.250 Å and LCD = 4.600 Å, and $\frac{V_{p,G}}{V_{p,PO}} = 0.988$.

What about the scenario shown in panel *C* of Fig. 3? Beyond small crystalline clusters, a regular icosahedron cluster of 13 argon atoms would require a cage of at least 10.2 Å in diameter. Hence, we can search for scenario *C* simply by screening through the LCD and PSDs with appropriate dimensions. Going through the members of the database along the diminishing values of positive deviations (where scenario *C* is expected), the first structure we come across that meets our criterion on the size of the cage is VFI with LCD of 11.55 Å. Figure 9 shows molecular visualizations of confined argon in VFI zeolite. As depicted in this figure, argon atoms indeed form a rather ordered structure along the channels with $\rho_a > \rho_{bulk}$. Not surprisingly, the ratio $\frac{V_{p,G}}{V_{p,PO}}$ is equal to 1.216 for VFI zeolite, indicating greater density of the confined argon compared to the bulk liquid.

Finally, we offer a speculative proposal on how the obtained data on the textural properties of zeolites and argon uptake can be used in practice. The uptake of argon reported here by a molecular simulation corresponds to the saturated adsorption capacity of a perfect, defect-free crystal. This property can provide a useful reference value to reflect on the quality of the experimental sample. Indeed, any discrepancy between the molecular simulation and experimental values can be interpreted as a result of the presence of some defects or structural transitions in a real sample.

For this proposal to work, we need to clearly identify specific constraints and assumptions under which we should perform such a comparison. Firstly, the remit of the current study is limited to the microporous materials, exhibiting simple Type I Langmuirian isotherm. Estimation of the pore volume in mesoporous materials with more complex adsorption behaviour is beyond the scope here, as it comes with a number of additional issues. In particular, the application of the Gurvich rule implies being able to observe a plateau region of the isotherm, where we can assume pores are filled with liquid-like argon. In heterogeneous mesoporous materials and materials featuring macropores, such a plateau is commonly not observed even very close to the saturation pressure. Hence, the Gurvich rule is not applicable. Alternatively, one uses the kernel methods (e.g., NLDFT) to extract pore size distribution (PSD) of the solid from the adsorption isotherm, and the pore volume is then obtained

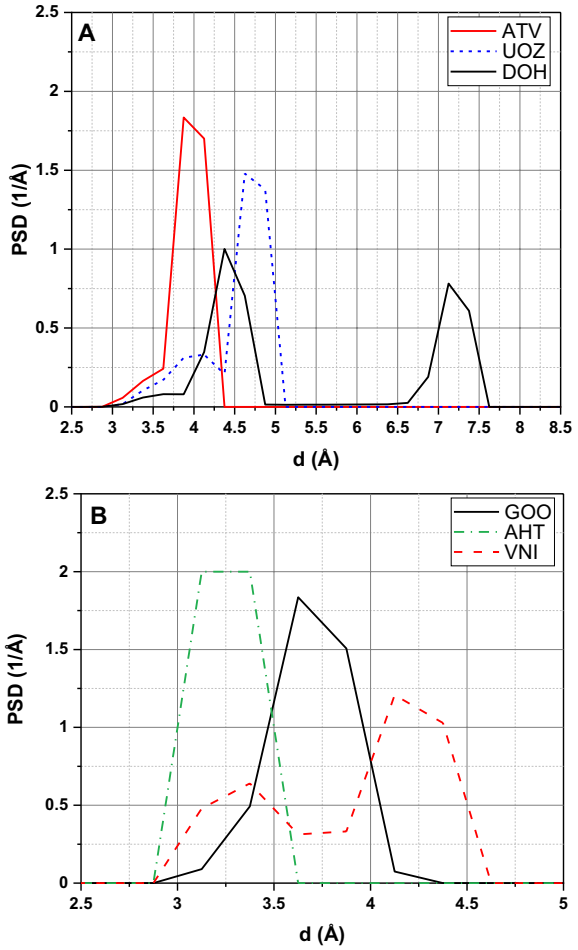

Fig. 6 Pore size distributions of three representative zeolites selected from Table 2 for topologies with **a** negative deviations and **b** positive deviations between $V_{p,PO}$ and $V_{p,G}$. PSDs of all zeolites from Table 2 are provided in Fig. S1

by integration over this PSD. The DFT-based methods also have their own scope and limitations and for a more comprehensive review on this issue we refer the reader to the report by Thommes et al. [2].

Secondly, the proposal above implies that molecular simulations can provide accurate predictions of adsorption in porous materials. The experimental argon sorption data on all-silica zeolites (either at 77 K or at 87 K) is very limited. As we show in the SI (Table S2), for the two materials, MFI and MEL, our molecular simulation results agree reasonably well with the reference simulation data and experiments in terms of the maximum loading of argon molecules per unit cell. Further validation of the simulation predictions is required using more extensive experimental data on high-quality samples.

Thirdly, for the purpose of this study we decided not to focus on the network-connectivity issues and all the data reported here is in terms of the total properties, rather than network-accessible properties. If the real sample of a zeolite is expected to have regions of the porous space, not accessible to argon, the values of the total pore volume and surface area obtained here from the computational methods cannot be compared directly to the experimental results. The Table S1 in the SI does provide network-accessible textural properties of zeolites for completeness, however these properties should be considered with caution, as the network-accessible properties are much more sensitive to the model of the probe molecule and zeolite, and to the thermal fluctuations of the zeolite framework. As an example of the impact of the thermal fluctuations on the size of the windows between the cages, we refer the reader to an early study by Deem et al. [27].

Instead, we suggest to apply our proposal to the structures that are fully accessible to argon. For these structures, the total probe-occupiable volume should be equal to the network-accessible probe-occupiable volume. Here we impose this constraint within 5% error. This leads to 127 zeolite structures out of 255 topologies that are reported by the IZA database. In Table S1 of the SI, these zeolites are marked as structures with an "argon-accessible network". Figure 10 shows the parity graph for $V_{p,PO}$ and $V_{p,G}$ for this group of zeolites.

In fact, at least 24 topologies from the all-silica zeolites shown in Fig. 10 are realized experimentally according to Wragg et al. [28] and therefore, it would be an interesting direction of research to obtain the experimental argon sorption data on these structures and compare them to the predictions from molecular simulations and geometric properties.

4 Conclusions

The outcomes of this investigation can be summarized as follows. As the objective of the study, we set to compare two definitions of the pore volume, one based on the Gurvich rule and one based on the purely geometric representation of the pore volume, using the all-silica versions of zeolite structures from the IZA database as a case study. In a situation where argon confined in a pore forms a liquid-like structure, the values of the pore volume from the two definitions should be consistent with each other. Intuitively, we expect that under the confinement of very narrow channels in microporous zeolite structures, the packing of argon molecules would significantly deviate from the bulk liquid structure. Surprisingly, we observed many scenarios and cases where while the packing of argon molecules was obviously not liquid-like (e.g. chains), the volume obtained from the Gurvich rule, was lower or higher than the geometric volume, depending on the actual packing. For the cases where the volume from the Gurvich rule agreed with the geometric volume (within some margin),

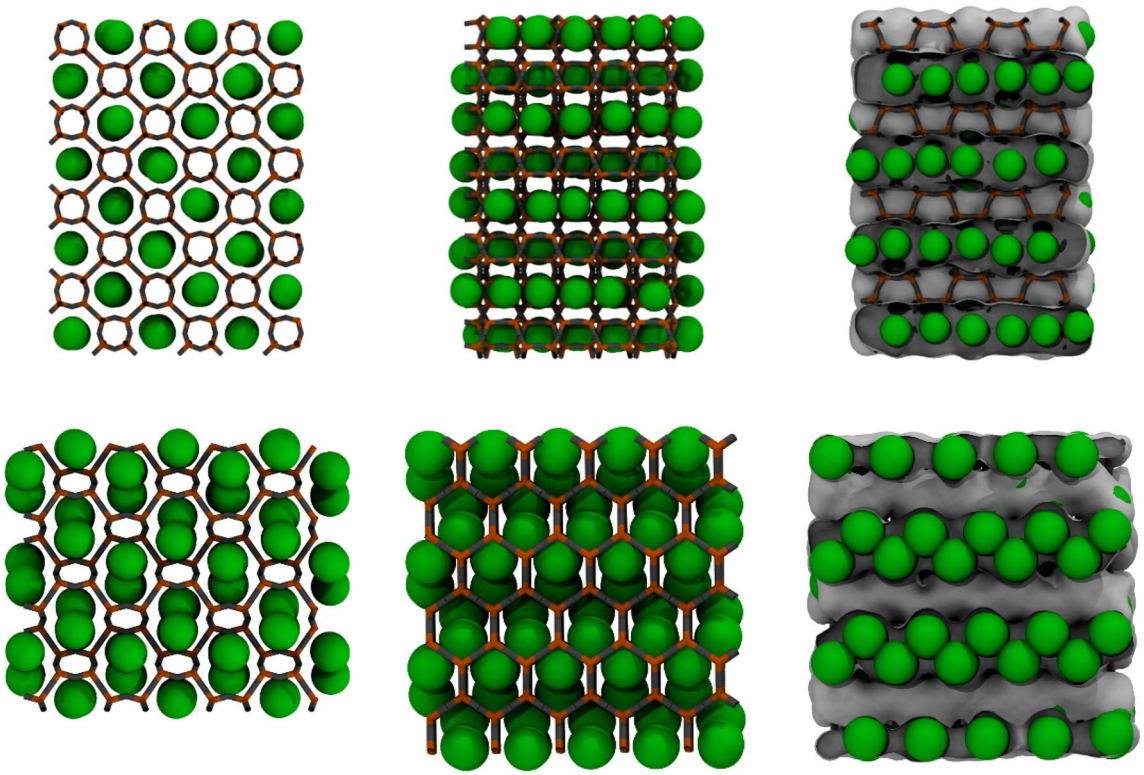

Fig. 7 Molecular visualizations of APD (top three panels) and ABW (bottom three panels) zeolite topologies from different perspectives. Colour scheme: zeolite framework is shown in grey (oxygen) and orange (silicon), argon is shown as green particles. In the panels on the right, the surface enclosing probe-occupiable volume is shown in grey. Molecular visualizations are generated by VMD software [31] (Color figure online)

this did not necessarily imply that the structure of the confined argon was liquid-like or had bulk liquid density. Our attempts to correlate the extent of disagreement between the Gurvich volume and geometric volume to some simple geometric features of the material, such as the value of the geometric volume itself, the pore size distribution or radial distribution function (analysis not shown here for brevity), proved to be challenging. It seems that more information is needed on the actual shape of the pores to make it possible to construct a model, which would predict in what way and to what extent the Gurvich volume would deviate from the reference geometric value for a particular structure. Overall, volume from the Gurvich rule agrees with the geometric volume within 25% error for 82% of the structures from the IZA database.

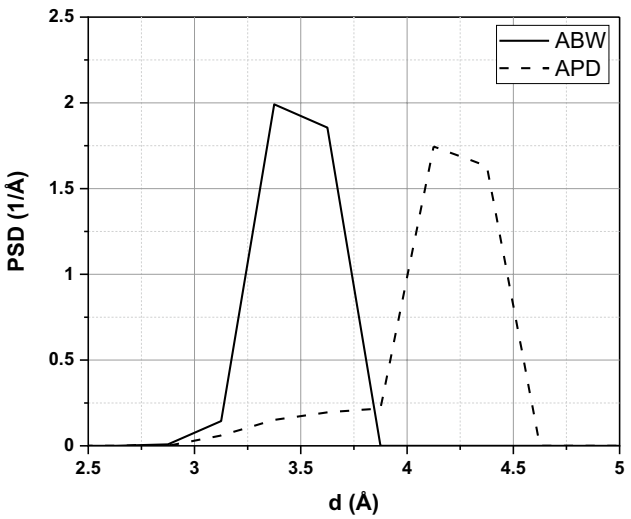

Fig. 8 Pore size distributions of APD and ABW zeolites

Another outcome of this study is a comprehensive compilation of the structural properties of all-silica zeolites from the IZA database. There is a growing interest in the synthesis and characterization of all-silica zeolites for a variety of adsorption applications [29, 30]. At the same time, argon at 87 K has been attracting attention as a more reliable, alternative probe to nitrogen in physical adsorption characterization [2]. Given these two co-current developments, we believe this compilation provides useful reference data on textural properties of all-silica zeolites, such as pore volume and surface area. However, taking full advantage of this data will require a more comprehensive

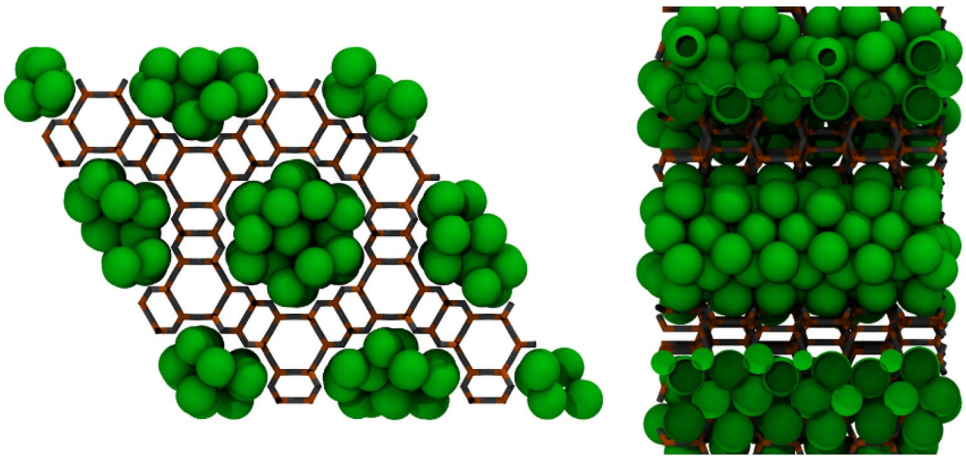

Fig. 9 Molecular visualizations of adsorbed phase in VFI zeolite forming icosahedron clusters of argon atoms. Molecular visualizations are generated by VMD software [31]

comparison of the molecular simulation and experimental data on argon sorption at 87 K in high-quality samples of these structures, which is currently lacking.

5 Supporting information

The Supporting Information is available free of charge on the journal website. This includes Table S1 summarizing the textural properties of 255 zeolites that are available in the Database of Zeolite Structures at the time of publication.

The complete set of simulation data including the original simulation setups and output files from Poreblazer and RASPA for the entire zeolite structures are available from our GitHub repository at: https://github.com/SarkisovGitHub/IZA_Zeolites.

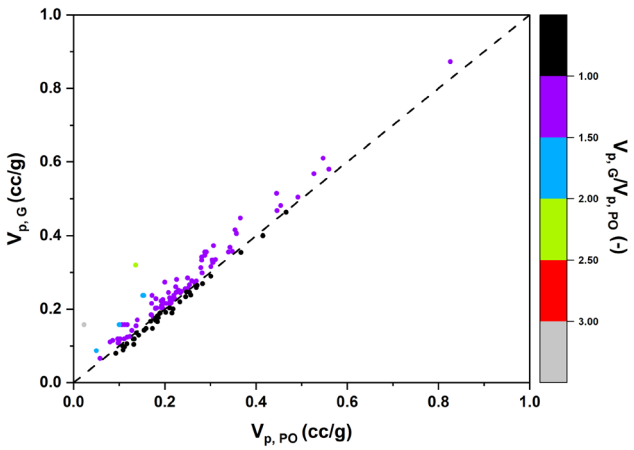

Fig. 10 Comparison of $V_{p,PO}$ and $V_{p,G}$ for zeolite topologies that are fully accessible to argon molecule (the probe-occupiable pore volume is equal to network-accessible probe-occupiable volume within 3% relative error)

Supplementary Information The online version contains supplementary material available at https://doi.org/10.1007/s10450-022-00364-w.

Acknowledgements We would like to thank Prof. Dr. Matthias Thommes for the comments and discussion on the practical challenges in zeolite characterization using argon sorption. The authors would like to acknowledge the assistance given by Research IT for the use of the Computational Shared Facility at The University of Manchester.

Declarations

Conflict of interest The authors declare that they have no conflict of interest.

References

1. Gurvich, L.: cited in SJ Gregg, KSW Sing, Adsorption, Surface Area and Porosity, Academic Press, London, p124, 1982. as. J. Phys. Chem. Soc. Russ **47**(1), 49–56 (1915)
2. Thommes, M., Kaneko, K., Neimark, A.V., Olivier, J.P., Rodriguez-Reinoso, F., Rouquerol, J., Sing, K.S.W.: Physisorption of gases, with special reference to the evaluation of surface area and pore size distribution (IUPAC Technical Report). Pure Appl. Chem. **87**(9–10), 1051–1069 (2015)

3. Islamoglu, T., Idrees, K.B., Son, F.A., Chen, Z., Lee, S.-J., Li, P., Farha, O.K.: Are you using the right probe molecules for assessing the textural properties of metal–organic frameworks? J. Mater. Chem. A **10**(1), 157–173 (2022)
4. Ongari, D., Boyd, P.G., Barthel, S., Witman, M., Haranczyk, M., Smit, B.: Accurate characterization of the pore volume in microporous crystalline materials. Langmuir **33**(51), 14529–14538 (2017)
5. First, E.L., Gounaris, C.E., Wei, J., Floudas, C.A.: Computational characterization of zeolite porous networks: an automated approach. Phys. Chem. Chem. Phys. **13**(38), 17339–17358 (2011)
6. Haldoupis, E., Nair, S., Sholl, D.S.: Pore size analysis of >250 000 hypothetical zeolites. Phys. Chem. Chem. Phys. **13**(11), 5053–5060 (2011)
7. Sarkisov, L., Bueno-Perez, R., Sutharson, M., Fairen-jimenez, D.: Material informatics with PoreBlazer v4.0 and CSD MOF database. Chem. Mater. **32**(23), 9849–9867 (2020)
8. Sarkisov, L., Harrison, A.: Computational structure characterisation tools in application to ordered and disordered porous materials. Mol. Simul. **37**(15), 1248–1257 (2011)
9. Willems, T.F., Rycroft, C.H., Kazi, M., Meza, J.C., Haranczyk, M.: Algorithms and tools for high-throughput geometry-based analysis of crystalline porous materials. Microporous Mesoporous Mater. **149**(1), 134–141 (2012)
10. Wilmer, C.E., Leaf, M., Lee, C.Y., Farha, O.K., Hauser, B.G., Hupp, J.T., Snurr, R.Q.: Large-scale screening of hypothetical metal-organic frameworks. Nat. Chem. **4**(2), 83–89 (2012)
11. Boyd, P.G., Woo, T.K.: A generalized method for constructing hypothetical nanoporous materials of any net topology from graph theory. CrystEngComm **18**(21), 3777–3792 (2016)
12. Earl, D.J., Deem, M.W.: Toward a database of hypothetical zeolite structures. Ind. Eng. Chem. Res. **45**(16), 5449–5454 (2006)
13. Pophale, R., Cheeseman, P.A., Deem, M.W.: A database of new zeolite-like materials. Phys. Chem. Chem. Phys. **13**(27), 12407–12412 (2011)
14. Ongari, D., Talirz, L., Jablonka, K.M., Siderius, D.W., Smit, B.:. Data-driven matching of experimental crystal structures and gas adsorption isotherms of metal-organic frameworks. ChemRxiv (2021)
15. Brandani, S., Mangano, E., Luberti, M.: Net, excess and absolute adsorption in mixed gas adsorption. Adsorption **23**(4), 569–576 (2017)
16. Farmahini, A.H., Krishnamurthy, S., Friedrich, D., Brandani, S., Sarkisov, L.: Performance-based screening of porous materials for carbon capture. Chem. Rev. **121**(17), 10666–10741 (2021)
17. Li, Y., Li, L., Yu, J.: Applications of zeolites in sustainable chemistry. Chemistry **3**(6), 928–949 (2017)
18. Valencia, S.: Zeolitic microporous materials and their applications. Molecules **26**(3), 730 (2021)
19. Baerlocher, C., McCusker, L.B.: Database of zeolite structures: http://www.iza-structure.org/databases/. International Zeolite Association (2021)
20. Johnson, J.K., Zollweg, J.A., Gubbins, K.E.: The Lennard-Jones equation of state revisited. Mol. Phys. **78**(3), 591–618 (1993)
21. Dubbeldam, D., Calero, S., Ellis, D.E., Snurr, R.Q.: RASPA: molecular simulation software for adsorption and diffusion in flexible nanoporous materials. Mol. Simul. **42**(2), 81–101 (2016)
22. Talu, O., Myers, A.L.: Reference potentials for adsorption of helium, argon, methane, and krypton in high-silica zeolites. Colloids Surf. A **187–188**, 83–93 (2001)
23. Zaccone, A.: Explicit analytical solution for random close packing in $d=2$ and $d=3$. Phys. Rev. Lett. **128**(2), 028002 (2022)
24. Schmidt, M., Löwen, H.: Phase diagram of hard spheres confined between two parallel plates. Phys. Rev. E **55**(6), 7228–7241 (1997)
25. Oğuz, E.C., Marechal, M., Ramiro-Manzano, F., Rodriguez, I., Messina, R., Meseguer, F.J., Löwen, H.: Packing confined hard spheres denser with adaptive prism phases. Phys. Rev. Lett. **109**(21), 218301 (2012)
26. Lemmon, E.W., Bell, I.H., Huber, M.L., McLinden, M.O.: (retrieved February 13, 2022). Thermophysical Properties of Fluid Systems. NIST Chemistry WebBook, NIST Standard Reference Database Number 69. P. J. Linstrom and W. G. Mallard. Gaithersburg MD, 20899, National Institute of Standards and Technology.
27. Deem, M.W., Newsam, J.M., Creighton, J.A.: Fluctuations in zeolite aperture dimensions simulated by crystal dynamics. J. Am. Chem. Soc. **114**(18), 7198–7207 (1992)
28. Wragg, D.S., Morris, R.E., Burton, A.W.: Pure silica zeolite-type frameworks: a structural analysis. Chem. Mater. **20**(4), 1561–1570 (2008)
29. Leon, S., Sastre, G.: Zeolite phase selectivity using the same organic structure-directing agent in fluoride and hydroxide media. J. Phys. Chem. C **126**(4), 2078–2087 (2022)
30. Mi, Z., Lu, T., Zhang, J.-N., Xu, R., Yan, W.: Synthesis of pure silica zeolites. Chem. Res. Chin. Univ. **38**(1), 9–17 (2022)
31. Humphrey, W., Dalke, A., Schulten, K.: VMD: visual molecular dynamics. J. Mol. Graph. **14**(1), 33–38 (1996)
32. Hirschfelder, J.O., Curtiss, C.F., Bird, R.B.: Molecular Theory of Gases and Liquids. Wiley, New York (1964)
33. Rappe, A.K., Casewit, C.J., Colwell, K.S., Goddard, W.A., Skiff, W.M.: UFF, a full periodic table force field for molecular mechanics and molecular dynamics simulations. J. Am. Chem. Soc. **114**(25), 10024–10035 (1992)